ApJL: Accepted November 11, 1998
Preprint typeset using LaTeX style emulateapj

THE PHYSICAL NATURE OF THE LYMAN LIMIT SYSTEMS

JASON X. PROCHASKA[1]
Department of Physics, and Center for Astrophysics and Space Sciences;
University of California, San Diego;
C–0424; La Jolla; CA 92093

ApJL: Accepted November 11, 1998

ABSTRACT

We analyze Keck HIRES observations of a Lyman limit system at $z = 2.652$ toward Q2231−00. These observations afford the most comprehensive study of the physical properties of a LL system to date. By comparing the ionic column densities for Fe^{+}, Fe^{++}, Si^{+}, and Si^{3+} against calculations derived from the CLOUDY software package, we have strictly constrained the ionization state of this system. This has enabled us to calculate accurate abundances of a Lyman limit system for the first time at $z > 2$, e.g., [Fe/H] $= -0.5 \pm 0.1$. We also derive a total hydrogen column density, $\log N(\mathrm{H}) = 20.73 \pm 0.2$, which is comparable to values observed for the damped Lyα systems.

The system is special for exhibiting CII* 1335 absorption, allowing an estimate of the electron density, $n_e = 6.5 \pm 1.3 \times 10^{-2}$ cm^{-3}. Coupling this measurement with our knowledge of the ionization state, we derive the following physical properties: (1) hydrogen volume density, $n_H = 5.9 \pm 1.2 \times 10^{-2}$ cm^{-3}, (2) path length, $\ell = 3 \pm 1.6$ kpc, and (3) ionizing intensity, $\log J_{912} = -20.22 \pm 0.21$. We point out that a number of the physical properties (e.g. [Fe/H], $N(\mathrm{H})$, n_H) resemble those observed for the damped Lyα systems, which suggests this system may be the photoionized analog of a damped system. The techniques introduced in this Letter should be applicable to a number of Lyman limit systems and therefore enable a survey of their chemical abundances and other physical properties.

Subject headings: quasars:individual (Q2231−00) — absorption lines — galaxies: abundances

1. INTRODUCTION

Observations of the Quasar Absorption Line (QAL) systems provide an efficient means for probing the physical conditions of the early universe. Intermediate resolution surveys have enabled accurate measurements on the evolution of the number density of the QAL systems, including the damped Lyα systems (Wolfe et al. 1986, Wolfe et al. 1995), the Lyman limit (LL) systems (Sargent, Steidel & Boksenberg 1989), and the Lyα forest clouds (Sargent et al. 1980). Until recently, the absence of a comprehensive physical description of the various QAL systems has limited the impact of these surveys. With the wealth of data afforded by echelle spectrographs on 10m class telescopes, one is now capable of making direct measurements of the physical properties of individual QAL systems and, in turn, the role of these systems in galaxy formation and the evolution of the early universe.

Over the past few years, observations of the damped Lyα systems – QAL systems with neutral hydrogen column densities $N(\mathrm{HI}) > 2 \times 10^{20}\,\mathrm{cm}^{-2}$ – have provided detailed measurements on their chemical composition, ionization state, dust content, metallicity, and kinematic characteristics (Pettini et al. 1994, Prochaska and Wolfe 1996, Lu et al. 1996, Prochaska & Wolfe 1997a). These observations present vital clues to galaxy formation theory. Thus far, little research has focused on the physical properties of the Lyman limit systems, QAL systems optically thick at the Lyman continuum. Owing to the challenges associated with accurately determining the ionization state of these partially ionized systems, their metallicity and chemical abundances have been poorly constrained. Steidel (1990) performed a survey of the physical properties of $z \approx 3$ LL systems, but the majority of his observations resulted only in limits to the abundances and other properties. With Keck, thus far researchers have focused on the kinematic characteristics of the MgII systems (Charlton & Churchill 1996), the majority of which are LL systems. Their efforts have provided keen insight into these systems at moderate redshift $z \approx 1$, but have been somewhat limited by difficulties in identifying their ionization state.

In this Letter, we present techniques aimed at determining the physical characteristics of a single LL system, including measurements of the ionization state, chemical abundances, electron density, and the intensity of ionizing radiation. While the results from this single LL system are not necessarily representative of all LL systems, the techniques outlined in this letter will be applicable to further LL studies, particularly when $N(\mathrm{HI}) > 10^{18}\,\mathrm{cm}^{-2}$. By applying these methods to a significant number of LL systems at high redshift we will investigate their chemical history, contrast their properties with those of the damped Lyα systems, and thereby probe physical conditions in the early universe. Section 2 presents the observations and measurements of the ionic column densities and the ionization state. In §3, we determine elemental abundances by making ionization corrections to the ionic column densities. We estimate the electron density, hydrogen volume density, and the intensity of ionizing radiation through an analysis of the fine structure CII* 1335 transition. Finally,

[1]Visiting Astronomer, W.M. Keck Telescope. The Keck Observatory is a joint facility of the University of California and the California Institute of Technology.

we provide a brief discussion and summary in §4.

2. OBSERVATIONS AND ANALYSIS

We observed Q2231−00 ($z_{em} = 3.02$) on the night of November 1, 1995 with HIRES (Vogt 1992) on the 10m W. M. Keck I Telescope for a total integration time of 2.5 hours. We used the C5 decker plate with $1.1''$ slit, standard 2×1 binning on the 2048×2048 Tektronix CCD, and the kv380 filter. For reduction and calibration of the data, we took a 360s exposure of the standard star BD +28 4211 and images of quartz and Th-Ar arc lamps. The data was reduced and wavelength calibrated with the software package written by Tom Barlow and continuum fit with the Iraf package *continuum*.

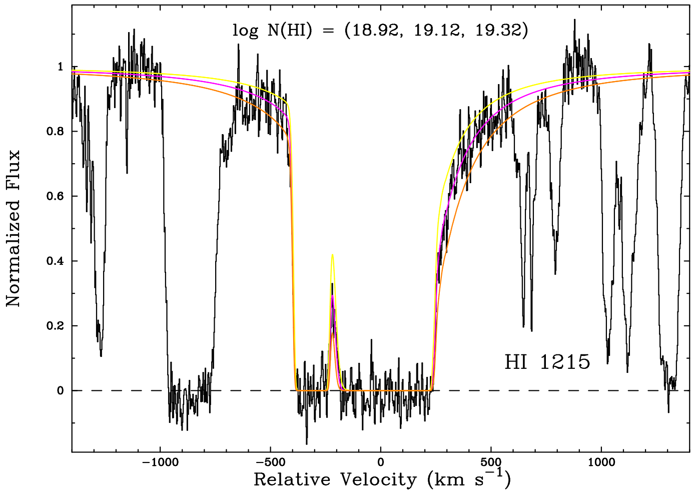

FIG. 1.— The Lyα profile of the Lyman limit system at $z = 2.652$ toward Q2231−00. The fit was performed with the VPFIT software package and corresponds to $\log N(\mathrm{HI}) = 19.12 \pm 0.15$ dex which includes an estimate to the continuum error.

A crucial component in the analysis of any QAL system is the neutral hydrogen column density, $N(\mathrm{HI})$. Figure 1 shows the HI Lyα profile for the LL system at $z = 2.652$ toward Q2231−00. While the line is heavily saturated, the damping wings are resolved and provide a good measurement of the $N(\mathrm{HI})$ value, $\log N(\mathrm{HI}) = 19.12$ dex. The curves in Figure 1 correspond to the line-profile fit (with estimated errors) derived from the VPFIT software package, kindly provided by R. Carswell and J. Webb. We include an estimated 0.15 dex error to the $N(\mathrm{HI})$ value due to the difficulty in determining the unabsorbed continuum flux in the Lyα forest.

Figure 2 presents the velocity profiles of the metal-line transitions observed for this LL system, with $v = 0$ corresponding to $z = 2.652$. The dotted lines designate regions of the profiles contaminated by other metal lines or Lyα forest clouds. The dashed vertical lines overplotted on the FeII 1608 transition indicate the velocity regions discussed below (Table 1). Note that the profiles track one another very closely in velocity space, *even across significantly different ionization states* (e.g. Fe^{+}, Fe^{++}, and Si^{3+}). As emphasized below, this observation is contrary to that typically observed for the damped Lyα systems (Prochaska and Wolfe 1996, Wolfe & Prochaska 1999). We have measured the ionic column densities from the unsaturated and mildly saturated line profiles by summing the apparent column density ($N_a(v) = m_e c \ln[I_c/I_a(v)]/\pi e^2 f \lambda$; Savage and Sembach 1991) over several velocity regions. This approach enables one to calculate ionic column densities as a function of velocity to search for variations in the ionization state, metallicity, and dust depletion. Table 1 lists the column densities for a number of the ions over four velocity regions and the total integrated column densities. We are particularly interested in the relative ionic column densities of Fe^{+}, Fe^{++}, Si^{+}, and Si^{3+} because the ratios Fe^{+}/Fe^{++} and Si^{+}/Si^{3+} constrain the ionization state of the system.

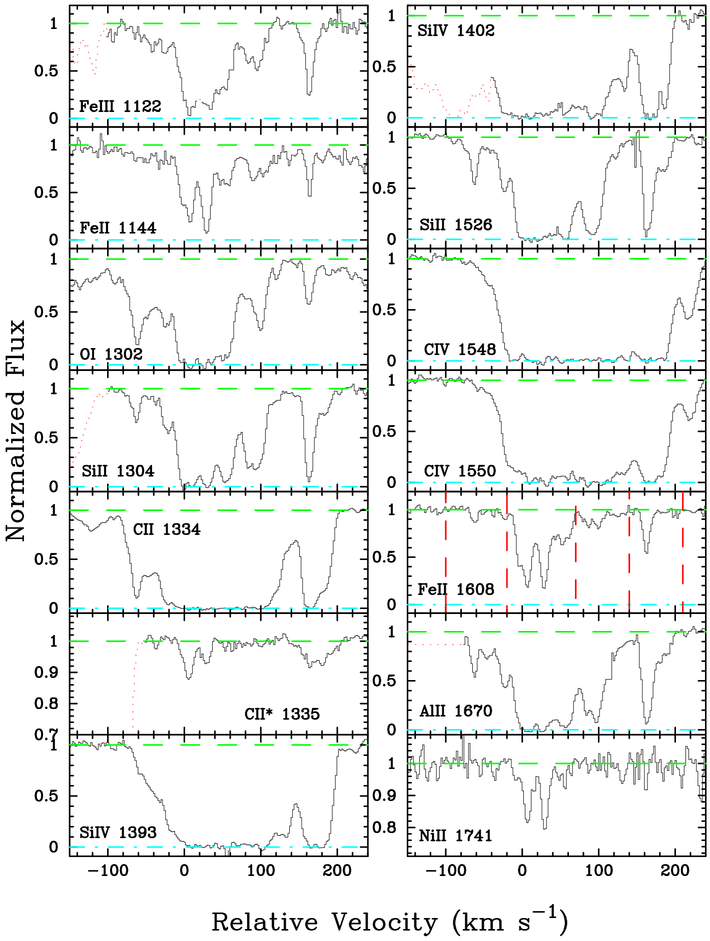

FIG. 2.— Velocity profiles of all the observed metal-line transitions. The dotted regions indicate portions of the profile contaminated by other absorption lines. The dashed vertical lines in FeII 1608 define the velocity regions discussed in the text.

To identify the ionization state of this LL system system, we have utilized the software package CLOUDY v90.04 (Ferland 1991). Figure 3 presents the predicted ionic column densities versus ionization parameter U for a model system assuming a Haardt-Madau spectrum (Haardt & Madau 1996), where

$$U \equiv \frac{\phi_{912}}{c n_H} = \frac{J_{912}}{4\pi h c n_H} = (2 \times 10^{-5}) \; \frac{J_{912}/10^{-21.5}}{n_H/\mathrm{cm}^{-3}} \quad (1)$$

with n_H the volume density of Hydrogen, and ϕ_{912} and J_{912} the flux and intensity of the incident radiation at 1 Rydberg. Note this is a modified definition of U; it was chosen to facilitate future comparisons with this work. The relative ionic column densities were calculated with the CLOUDY package assuming $N(\mathrm{HI}) = 10^{19.12}\,\mathrm{cm}^{-2}$, intrinsic solar abundances, and $[\mathrm{Fe/H}] = -0.5$ dex. The dashed vertical lines denote the range of U values consistent with the $\mathrm{Fe}^+/\mathrm{Fe}^{++}$ ratio (0.40 ± 0.05 dex) and the dotted line indicates the U value corresponding to the upper limit on the $\mathrm{Si}^+/\mathrm{Si}^{3+}$ ratio (i.e. a lower limit to U). These observations imply $\log U = -2.23 \pm .21$, which is the most accurate determination of U in a LL system to date.

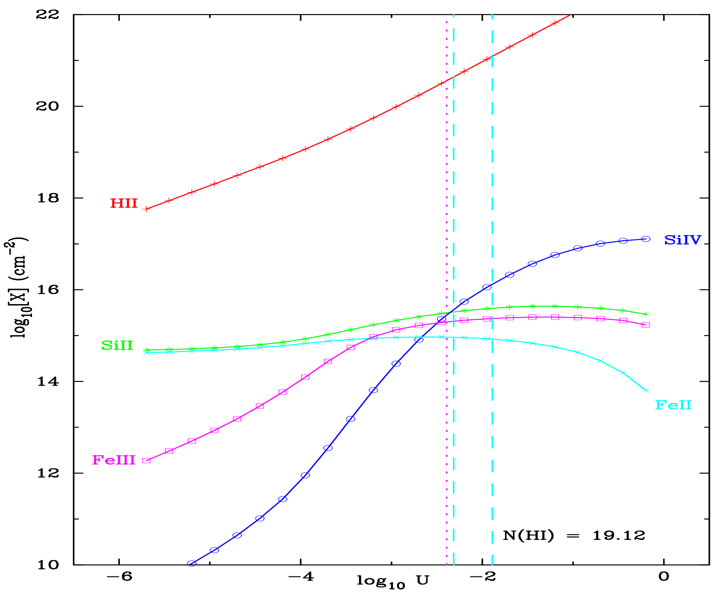

FIG. 3.— The results from a series of CLOUDY calculations (Ferland 1991) assuming a Haardt-Madau ionizing spectrum and $\log N(\mathrm{HI}) = 19.12$. Plotted are the calculated mean ionic column densities (assuming intrinsic solar abundances and $[\mathrm{Fe/H}] = -0.5$) versus a modified ionization parameter, U, as defined in the text. The vertical dashed lines indicate the observed $\mathrm{Fe}^+/\mathrm{Fe}^{++}$ ratio (with errors) and the dotted vertical line is a lower limit to the ionization parameter determined from the upper limit to the $\mathrm{Si}^+/\mathrm{Si}^{3+}$ ratio.

3. PHYSICAL PROPERTIES

In the previous section, we presented an accurate measurement of the system's ionization state by comparing the observed ionic column densities of H^0, Fe^+, Fe^{++}, Si^+, and Si^{3+} with the predicted results from a calculation performed with the CLOUDY software package. We find the system is highly ionized with ionization fraction, $x \equiv \mathrm{H}^+/\mathrm{H} = 0.97 \pm 0.02$. This implies that the total Hydrogen column density, $\log N(\mathrm{H}) = 20.73 \pm 0.2$, is comparable to that observed in the damped Lyα systems. This value is similar to the estimates from Steidel (1990) for his sample of LL systems. By making the appropriate ionization corrections from the CLOUDY results, we derive the elemental abundances of this system. The logarithmic abundance of element X relative to Hydrogen and normalized to solar abundances (Anders & Grevesse 1989), $[\mathrm{X/H}] = \log[\mathrm{N(X)/N(H)}] - \log[\mathrm{X/H}]_\odot$, are listed in the last column of Table 1. We find $[\mathrm{Fe/H}] = -0.5$ dex which is higher than the typical damped Lyα system and considerably higher than any other estimate to the abundances of a LL system at $z > 2$.

To gauge the accuracy with which we have determined the ionization state and thereby the chemical abundances, we have investigated the effects of varying $N(\mathrm{HI})$ and the shape of the input spectrum. We find that the 0.15 dex uncertainty in the $N(\mathrm{HI})$ value lends to less than a 0.1 dex uncertainty in [Fe/H] and the majority of other elemental abundances, including the $N(\mathrm{H})$ value. Furthermore, we considered the effects of a steeper spectrum (e.g. a Bregman-Harrington spectrum) and find a similar variation in the measured abundances. Examining the relative abundances of this system, we observe little departure from the Solar abundance pattern. There is, however, evidence for an overabundance of Si/Fe (the lower limit to [Si/H] is quite conservative given the degree of saturation in the Si profiles) and an underabundance of Ni/Fe as observed in the majority of the damped Lyα systems. In the damped systems, this pattern is typically interpreted as the result of dust depletion and/or TypeII supernovae enrichment. Unfortunately, the SII 1253 and SII 1259 profiles in this system are blended with Lyα forest clouds for the [S/Fe] measurement is sensitive to both of these interpretations.

The detection of the fine structure CII* 1335 transition allows further insight into the physical characteristics of this system. The fine structure line can be excited by several processes, but for a highly ionized system at this redshift, electron collisions dominate (Morris et al. 1986). Therefore, the observed $N(\mathrm{CII}^*)/N(\mathrm{CII})$ ratio provides a measure of the electron density via: $N(\mathrm{CII}^*)/N(\mathrm{CII}) = 3.9 \times 10^{-2}\, n_e \, [1 + (0.22 n_p/n_e)]$. Unfortunately the $N(\mathrm{CII}^*)/N(\mathrm{CI}$ ratio cannot be measured directly because the CII 1334 profile is saturated over the velocity region where the CII* absorption is detected[2]. We can accurately estimate the $N(\mathrm{CII}^*)/N(\mathrm{CII})$ ratio, however, provided the assumption

[2]We expect the absorption in Reg4 ($v \approx 170\ \mathrm{km\,s^{-1}}$) for the CII* 1335 transition is due to an intervening Lyα forest cloud and restrict the analysis to the absorption features in Reg2 ($v \approx 20\ \mathrm{km\,s^{-1}}$).

TABLE 1
IONIC COLUMN DENSITIES AND ABUNDANCES

Ion	λ	Reg1[a]	Reg2[b]	Reg3[c]	Reg4[d]	TOT	[X/H]
HI	1215	...	...	...	19.12 ± 0.2		
CII	1334	14.24 ± 0.01	15.41 ± 0.08[e]	> 14.76	14.42 ± 0.03	> 15.41	> -0.85
CII*	1335	...	12.90 ± 0.03	...	...	...	
OI	1302	14.49 ± 0.02	> 15.20	14.22 ± 0.02	13.82 ± 0.02	> 15.33	> -0.6
AlII	1670	12.35 ± 0.01	> 13.80	12.88 ± 0.02	12.67 ± 0.02	> 13.84	> -0.75
SiII	1304	13.58 ± 0.02	> 14.87	14.18 ± 0.01	14.03 ± 0.02	> 15.02	> -0.55
SiIV	1402	...	> 14.50	> 14.21	> 14.09	> 14.78	
FeII	1608	12.96 ± 0.08	14.34 ± 0.01	13.38 ± 0.03	13.43 ± 0.03	14.44 ± 0.05	-0.5 ± 0.1
FeIII	1122	13.71 ± 0.04	14.69 ± 0.03	13.86 ± 0.03	13.83 ± 0.03	14.84 ± 0.02	
NiII	1741	...	...	...	...	13.36 ± 0.04	-0.78 ± 0.05

[a]Velocity region spanning: -100 km s^{-1} $< v <$ -20 km s^{-1}
[b]Velocity region spanning: -20 km s^{-1} $< v <$ 70 km s^{-1}
[c]Velocity region spanning: 70 km s^{-1} $< v <$ 140 km s^{-1}
[d]Velocity region spanning: 140 km s^{-1} $< v <$ 210 km s^{-1}
[e]This value was obtained with the method described in §3

that the CII 1334 and FeII 1608 profiles track one another in velocity space. Low-ion profiles always track one another in the damped Lyα systems (e.g. Prochaska and Wolfe 1996, Lu et al. 1996) and one notes *all* of the transitions – irrespective of ionization state – trace one another in this system. Our approach, then, is (1) to measure N(CII)/N(FeII) in Reg4 where the effects of saturation are minimal and (2) correct a N(FeII) measurement in Reg2 by the N(CII)/N(FeII) ratio to estimate N(CII) in this velocity region. We find $N(\mathrm{CII}) = 15.41 \pm 0.08\,\mathrm{cm}^{-2}$ and correspondingly, $N(\mathrm{CII}^*)/N(\mathrm{CII}) = 3.09 \pm 0.75 \times 10^{-3}$. Assuming $n_p/n_e \approx 1$ for this highly ionized system this yields an electron density, $n_e = 6.5 \pm 1.3 \times 10^{-2}\,\mathrm{cm}^{-3}$.

The n_e value coupled with our knowledge of the ionization state enables an estimate of the hydrogen volume density and the intensity of the ionizing radiation. Ignoring the contribution to n_e from metals (a reasonable assumption when $x \approx 1$) and adopting $N(\mathrm{He}^+)/N(\mathrm{He}) = 0.9$ and $N(\mathrm{He}^{++})/N(\mathrm{He}) = 0.1$ from the CLOUDY calculations, we find $n_H = 5.9 \pm 1.2 \times 10^{-2}\,\mathrm{cm}^{-3}$. With $N(\mathrm{H}) \approx 10^{20.73}\,\mathrm{cm}^{-2}$, this implies a path length $\ell \equiv N(\mathrm{H})/n_H \approx 3 \pm 1.6$ kpc. While this length is rather uncertain ($>50\%$ statistical error) and does not account for clumping along the sightline, it is still one of the most meaningful size estimates of a QAL system to date. The ionizing intensity, J_{912}, is easily determined by inverting Equation 1: $\log J_{912} = -20.22 \pm 0.21$ which is higher (a factor of $5-10$) than typical estimates from the Proximity Effect (Lu et al. 1991), but not unreasonably high. Perhaps there is a source of local ionizing radiation (e.g. supernovae, OB stars) in addition to the extragalactic background radiation. Finally, consider the kinematic characteristics of this LL system. First note that the width of the profile spans nearly 200 km s^{-1} . Second, we observe that the strongest absorption feature lies at the left edge of the profile and the optical depth decreases monotonically towards positive velocity. This edge-leading asymmetric trait is characteristic of that observed in the damped Lyα systems (Prochaska & Wolfe 1997b, Prochaska & Wolfe 1998). Contrary to the damped Lyα systems, however, the low-ion profiles trace very closely the high-ion profiles (Si^{3+} and Fe^{++}). This indicates the various ionization states arise from the same regions within the system. Interestingly, one observes a similar correspondence between the line profiles of multiple ionization states in the ISM (Savage et al. 1997). A future survey will determine if a large sample of LL systems exhibit similar traits.

4. SUMMARY AND CONCLUSIONS

We have presented techniques for accurately determining the ionization state of a LL system. The technique requires the measurement of multiple ionization stages of a single element – in this case $\mathrm{Fe}^+/\mathrm{Fe}^{++}$ – an estimate of N(HI) and a series of calculations with the CLOUDY software package. It should be applicable to a number of high redshift LL systems and will enable a survey of their elemental abundances. For this system, we find an ionization fraction $x = 0.97 \pm 0.02$ and a corresponding Iron abundance, $[\mathrm{Fe/H}] = -0.5 \pm 0.1$ dex. The overall abundance pattern resembles that observed in the damped Lyα system possibly suggesting an underlying depletion pattern or TypeII SN enrichment. This system is unusual for exhibiting CII* 1335 absorption which provides one with an estimate of the electron density ($n_e = 6.5 \times 10^{-2}\,\mathrm{cm}^{-3}$). Our knowledge of the ionization state allows estimates of the hydrogen volume density ($n_H = 5.9 \times 10^{-2}\,\mathrm{cm}^{-3}$), the intensity of the ionizing radiation ($\log J_{912} = -20.22$), and the path length through the system $\ell = 3 \pm 1.6$ kpc.

It is instructive to compare this LL system with the properties of the damped Lyα systems. For example, we note the derived N(H) and n_H values are similar to those observed for the damped systems. In fact, if it were not for the high intensity of ionizing radiation, this system would be primarily neutral with $N(\mathrm{HI}) > 2 \times 10^{20}\,\mathrm{cm}^{-2}$. The observed abundances and kinematic characteristics further argue for this interpretation. It will be exciting to investigate the connection between other LL systems and the damped Lyα systems through a survey of LL systems at $z > 2$. This research will help develop a better understanding of the connection between the QAL systems and galaxy formation. In addition, a direct comparison with numerical simulations may provide insight into the nature of protogalaxies in the early universe.

We wish to acknowledge A. Wolfe, S. Burles and F. Hamann for helpful comments. We would also like to thank Bob Carswell and John Webb for kindly providing the VPFIT package, Piero Madau for providing an electronic version of their UVB spectrum and G. Ferland for developing and distributing CLOUDY. We thank T. Barlow for developing and providing the HIRES data reduction package. Finally, this work could not have been carried out without the helpful support of the Keck observing staff. JXP was partially supported by NASA grant NAGW-2119 and NSF grant AST 86-9420443.

REFERENCES

Anders, M.V., & Grevesse, N. 1989, Geochim. Cosmo. Acta, 53, 197
Bregman, J.N. & Harrington, J.P. 1986, ApJ, 309, 833
Charlton, J.C. & Churchill, C.W. 1996, ApJ, 465, 631
Ferland, G. J. 1991, Ohio State Internal Report 91-01
Haardt, F. & Madau, P. 1996, ApJ, 461, 20
Lu, L., Wolfe, A.M., & Turnshek, D.A. 1991, ApJ, 367, 19
Lu, L., Sargent, W.L.W., Barlow, T.A., Churchill, C.W., & Vogt, S. 1996b, ApJS, 107, 475
Morris, S.L, Weymann, R.J., Foltz, C.B., Turnshek, D.A., Shectman, S., Price, C., & Boronson, T.A. 1986, ApJ, 310, 40
Pettini, M., Smith, L. J., Hunstead, R. W., and King, D. L. 1994, ApJ, 426, 79
Prochaska, J. X. and Wolfe, A. M. 1996, ApJ, 470, 403
Prochaska, J. X. & Wolfe, A. M. 1997, ApJ, 474, 140
Prochaska, J. X. & Wolfe, A. M. 1997, ApJ, 486, 73
Prochaska, J.X. & Wolfe, A.M. 1998, ApJ, in press
Sargent, W.L.W., Young, P.J., Boksenberg, A., & Tytler, D. 1980, ApJS, 42, 41
Sargent, W.L.W., Steidel, C.C., & Boksenberg, A. 1989, ApJS, 69, 703
Savage, B. D. and Sembach, K. R. 1991, ApJ, 379, 245
Savage, B.D., Sembach, K.R., & Lu, L. 1997, AJ, 113, 2158
Steidel, C.C. 1990, ApJS, 74, 37
Vogt, S. S. 1992, in ESO Conf. and Workshop Proc. 40, High Resolution Spectroscopy with the VLT, ed. M.-H. Ulrich (Garching: ESO), p. 223
Wolfe, A. M., Turnshek, D. A., Smith, H. E. and Cohen, R. D. 1986, ApJ, 61, 249
Wolfe, A. M., Lanzetta, K. M., Foltz, C. B., and Chaffee, F. H. 1995, ApJ, 454, 698
Wolfe, A.M. & Prochaska, J.X. 1999, ApJ, submitted